Radiat Environ Biophys (2016) 55:381–391
DOI 10.1007/s00411-016-0652-7

ORIGINAL ARTICLE

Radiobiological influence of megavoltage electron pulses of ultra-high pulse dose rate on normal tissue cells

Lydia Laschinsky[1,2,3] · Leonhard Karsch[1] · Elisabeth Leßmann[2] · Melanie Oppelt[1,2,4] · Jörg Pawelke[1,2] · Christian Richter[1,2] · Michael Schürer[1] · Elke Beyreuther[2]

Received: 16 November 2015 / Accepted: 9 May 2016 / Published online: 19 May 2016

Abstract Regarding the long-term goal to develop and establish laser-based particle accelerators for a future radiotherapeutic treatment of cancer, the radiobiological consequences of the characteristic short intense particle pulses with ultra-high peak dose rate, but low repetition rate of laser-driven beams have to be investigated. This work presents in vitro experiments performed at the radiation source ELBE (Electron Linac for beams with high Brilliance and low Emittance). This accelerator delivered 20-MeV electron pulses with ultra-high pulse dose rate of 10^{10} Gy/min either at the low pulse frequency analogue to previous cell experiments with laser-driven electrons or at high frequency for minimizing the prolonged dose delivery and to perform comparison irradiation with a quasi-continuous electron beam analogue to a clinically used linear accelerator. The influence of the different electron beam pulse structures on the radiobiological response of the normal tissue cell line 184A1 and two primary fibroblasts was investigated regarding clonogenic survival and the number of DNA double-strand breaks that remain 24 h after irradiation. Thereby, no considerable differences in radiation response were revealed both for biological endpoints and for all probed cell cultures. These results provide evidence that the radiobiological effectiveness of the pulsed electron beams is not affected by the ultra-high pulse dose rates alone.

Keywords Laser-driven radiotherapy · Cell response to electron beams · Pulsed irradiation · Ultra-high pulse dose rate · Normal tissue cell culture

Introduction

The new acceleration of charged particles by high-intensity lasers has been proposed as a next generation of compact particle accelerators. The progress in developing laser-based acceleration technology during the last decade opened their serious consideration for medical application in cancer radiotherapy (e.g. Ledingham et al. 2007; Linz and Alonso 2007; Lundh et al. 2012). The therapeutically relevant parameters of laser-accelerated particle beams differ from those provided by conventional clinical electromagnetic accelerators. Laser-driven beams are characterized by short pulses (duration in the range of ps) with a low repetition rate (typically a few Hz), but with very high pulse dose, resulting in an ultra-high peak dose rate of more than 10^{11} Gy/min exceeding those of conventional beams by several orders of magnitude (Beyreuther et al. 2010; Kraft et al. 2010; Rigaud et al. 2010; Yogo et al. 2011; Laschinsky et al. 2012). Besides the compulsory development of high-power laser systems and laser targets to generate particle beams of sufficient quality for medical application, also the radiobiological consequences of radiation pulses with ultra-high peak dose rate have to be investigated.

✉ Elke Beyreuther
E.Beyreuther@hzdr.de

[1] OncoRay – National Centre for Radiation Research in Oncology, Faculty of Medicine and University Hospital Carl Gustav Carus, Technische Universität Dresden, Fetscherstr. 74, PF 41, 01307 Dresden, Germany

[2] Institute of Radiation Physics, Helmholtz-Zentrum Dresden – Rossendorf (HZDR), Bautzner Landstraße 400, P.O. Box 510119, 01314 Dresden, Germany

[3] Present Address: Menarini – Von Heyden GmbH, Leipziger Straße 7 – 13, 01097 Dresden, Germany

[4] Present Address: Quintiles GmbH, Hugenottenallee 167, 63263 Neu-Isenburg, Germany

The influence of ultra-high pulse dose rates (UHPDR) has been investigated with conventional, i.e. not laser-driven, accelerators that were able to deliver a dose of few gray in single electron pulses, resulting in pulse dose rates between 10^8 Gy/min and 10^{13} Gy/min (Berry and Stedeford 1972; Purrott and Reeder 1977; Michaels et al. 1978; Purdie et al. 1980; Cygler et al. 1994; DeVeaux et al. 2006; Acharya et al. 2011). Radiation response studies have been performed for diverse biological endpoints (chromosomal aberrations, cell survival), cell cultures (human, mouse, bacteria), electron energies (few hundreds keV up to several MeV) and reference radiation qualities (X-rays, γ-rays and electron beams in a broad energy range). For the majority of these studies, no impact of a UHPDR to the radiobiological outcome was revealed (Berry and Stedeford 1972; Purrott and Reeder 1977; Purdie et al. 1980; Cygler et al. 1994; DeVeaux et al. 2006). However, an ascertainable influence was attributed to the duration and number of multiple electron pulses (Acharya et al. 2011) and was detected under reduced oxygen tension (Michaels et al. 1978). With the availability of particle beams by high-intensity lasers, first radiobiological in vitro experiments regarding UHPDR with laser-accelerated electron (Rigaud et al. 2010; Laschinsky et al. 2012; Labate et al. 2013) and proton beams (Kraft et al. 2010; Yogo et al. 2011; Bin et al. 2012; Doria et al. 2012; Zeil et al. 2013) were performed in the past few years. Up to now, only one study is known (Laschinsky et al. 2012) where the radiation response of laser-accelerated and a conventional beam of similar radiation quality (apart from the ultra-high pulse dose rate) was directly compared and where more than one cell line and more than one biological endpoint was investigated. In this study, cell survival and residual DNA double-strand breaks (DSB) have beam determined for a tumour (FaDu) and a normal tissue (184A1) cell line by irradiation of cells with laser-accelerated electron beams at the JETI (Jena Titanium:Sapphire) laser system and with conventional, quasi-continuous electron beams at a clinical linear accelerator (LINAC). The dose–response curves showed no significant difference in the radiobiological effectiveness in three of four cases, i.e. for clonogenic survival of FaDu and 184A1 as well as for residual DNA DSB for FaDu. However, by analysing residual DNA DSB for the normal tissue cell line 184A1, a significantly reduced radiobiological effectiveness of laser-accelerated, short-pulsed electron beams was detected in comparison with conventional, quasi-continuous electron beams.

Considering the last mentioned fact, the aim of this study was to perform continuative investigations to determine the influence of the laser-accelerator-specific, ultra-high pulse dose rate by using the radiation source ELBE (Electron Linac for beams with high Brilliance and low Emittance), (Gabriel et al. 2000). This superconducting electromagnetic accelerator allows the setting of the time structure and pulse dose of monoenergetic megavoltage electron beams over several orders of magnitude. Therefore, the beam pulse structures of both high-intensity laser accelerator and clinical LINAC can be imitated at the radiation source ELBE. In addition, the radiobiological response of cells to electron beams of different pulse structures can be compared directly without the interference by differences in other beam properties (e.g. energy spectrum) and by different set-ups, dosimetry systems and environmental conditions from separated experimental sessions at two accelerators (Beyreuther et al. 2015). Hence, the normal tissue cell line 184A1 studied in the previous experiment at the JETI laser accelerator (Laschinsky et al. 2012) was investigated at the ELBE electron beam to ascertain the influence of the UHPDR on the clonogenic survival and the number of residual DNA DSB that remain 24 h after irradiation. As for the JETI study, the latter was investigated by counting double-positive γ-H2AX and 53BP1 fluorescence foci as signalling molecules for unrepaired DSB, being aware that the loss of these foci is not necessarily linked to DSB repair (as discussed in more detail in Beyreuther et al. 2009). Besides cell line 184A1, the dose rate influence was also investigated on the normal human, primary fibroblasts HDF and F153 by analysing residual DNA DSB.

Materials and methods

Cell culture

One human cell line and two human primary fibroblasts were used in the present irradiation experiments. The normal tissue mammary gland breast epithelium cell line 184A1 (ATCC, CRL-8798) was established from a mammoplasty of a 21-year-old female (Stampfer and Bartley 1985). These cells were developed as continuous cell line, which appears to be immortal but not malignant (Stampfer and Bartley 1985). The cultivation of 184A1 cells was performed by using serum-free mammary epithelia basal medium supplemented with MEGM SingleQuots® (both from Lonza), 50 mg/ml prostaglandin E1 (Calbiochem) and 5 µg/ml human apo-transferrin (Sigma-Aldrich). The normal human neonatal foreskin-derived dermal fibroblasts HDF (CellSystems, FC-0001) were maintained in FibroLife® basal medium supplemented with FibroLife® LifeFactors kit and 1.25 ml HLL supplement (all from CellSystems). The normal human fibroblasts F153 were kindly provided by Prof. Dikomey (Universitätsklinikum Hamburg-Eppendorf, laboratory for radiobiology and experimental radiooncology) and were cultured in Dulbecco's minimum essential medium with 4.5 g/l

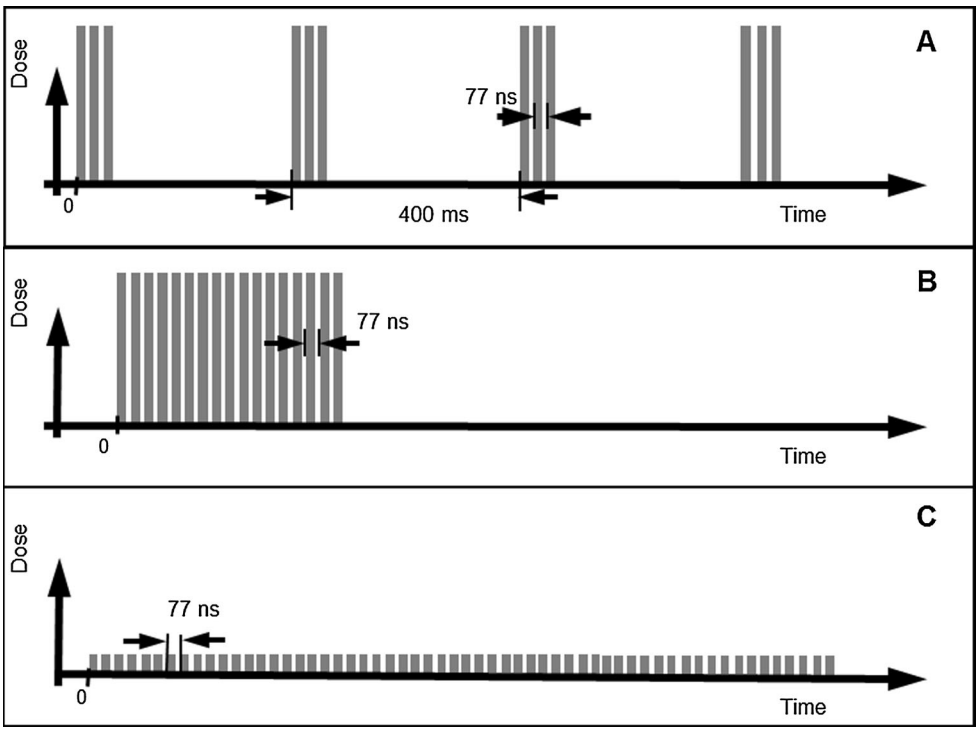

Fig. 1 Schematic illustration of the radiobiologically investigated electron pulse regimes at the radiation source ELBE. **a** UHPDR-LF pulse regime comparable to laser-accelerated electrons at the laser system JETI, **b** UHPDR-HF pulse regime, **c** quasi-continuous electron beam analogue to dose delivery by a clinical LINAC

stable glutamin (Biochrom) containing 10 % FBS (Sigma-Aldrich), 1 mM sodium pyruvate, 20 mM HEPES, 1 % 100× non-essential amino acids (all from PAA) and 1 % penicillin/streptomycin (Biochrom). All cell cultures were routinely checked for mycoplasma using Venor®GeM (Biochrom). Cells were maintained at 37 °C, 5 % CO_2 and in a 95 % humidification.

For the purpose of experiment comparison, 3.0×10^5 exponentially growing cells were seeded 2 days before irradiation in petri dishes with a diameter of 35 mm (Greiner bio one). One day before irradiation, the cell culture medium was changed. Directly before irradiation, each cell sample was completely filled up with cell culture medium and enclosed with sterile Parafilm® (Merck; 24 h in 80 % ethanol and at least 2 h UV light) to allow an upright cell sample exposure at the horizontal ELBE electron beam. In addition, for each endpoint and radiation quality a sufficient number of cell samples were prepared for sham irradiation and were used as control samples.

Electron pulse regimes for irradiation at ELBE

The superconducting linear electron accelerator ELBE at HZDR (Gabriel et al. 2000) was used for the electron irradiation experiments investigating three beam pulse regimes. ELBE provided a 20-MeV pulsed electron beam with 5-ps-long micropulses (bunches) at a fixed micropulse frequency of 13 MHz. The time structure of the ELBE electron beam can be modulated additionally by merging a variable number of up to 2^{31} electron bunches in macropulses. The time interval between these macropulses can be varied between 1 ms to several minutes, modulating the basic bunch frequency of 13 MHz by a superimposed macropulse frequency.

Three electron pulse regimes, schematically pictured in Fig. 1, were applied by varying the number and frequency of the electron macropulses as well as the bunch charge, i.e. the delivered dose per pulse. The first pulse regime named ultra-high pulse dose rate at low frequency (UHPDR-LF, Fig. 1a) was set up to mimic the electron beam delivery at the JETI laser accelerator (cf. Table 1). The ELBE electron beam was tuned to maximum bunch charge. The pulse dose of few mGy was achieved by combining the electron bunch charge of three micropulses provided at the basic frequency of 13 MHz to one macropulse. Macropulses were delivered at the same low frequency of 2.5 Hz as given by the laser system JETI, resulting in a mean dose rate of ~0.4 Gy/min comparable to those at JETI. In order to avoid the influence of the low mean dose rate, electron micropulses of maximum bunch charge were delivered at high frequency of 13 MHz in a single macropulse. This second electron pulse regime allowed the delivery of the desired total dose within the technical minimum irradiation time at ELBE and was termed ultra-high pulse dose rate at high frequency (UHPDR-HF, Fig. 1b). The third regime named quasi-continuous (Fig. 1c) mimicked the electron beam delivery of the clinical LINAC utilized in the previous experiments for

Table 1 Electron beam parameters of the three pulse regimes at the radiation source ELBE, the laser accelerator JETI and the clinical LINAC

	ELBE			JETI laser acc.[a]	Clinical LINAC[a]
	Quasi-continuous	UHPDR			
		HF	LF		
Beam energy	20 MeV	20 MeV	20 MeV	3–20 MeV	6 MeV
Pulse frequency	13 MHz	13 MHz	2.5 Hz[b]	2.5 Hz	50 Hz[b]
Pulse length	5 ps	5 ps	5 ps	1 ps	4 μs[b]
Dose per pulse	~nGy	~mGy	~mGy	~mGy	~mGy[b]
Irradiation time	~min	≤1 ms	≤30 min	≤33 min	~min
Mean dose rate/Gy min^{-1}	~4	~10^{6}	~0.4	~0.4	~3
Pulse dose rate/Gy min^{-1}	~10^{4}	~10^{10}	~10^{10}	~10^{11}	10^{4b}

[a] Beam parameters from Laschinsky et al. 2012

[b] Macropulse parameter is given

comparison irradiation to the laser-accelerated electron exposure. Therefore, electron micropulses of low bunch charge were tuned without any macropulse modulation, resulting in a mean dose rate of 4 Gy/min comparable to those of a clinical LINAC (cf. Table 1). It has to be noted that the clinical LINAC technically delivered a pulsed beam. Here, electron bunches provided at a frequency of approximately 3 GHz and with a bunch length in the ps range were superimposed by macropulses of 50 Hz frequency and 4 μs pulse length. Due to the low micropulse dose of approx. $8{\cdot}10^{-8}$ Gy and short bunch length in combination with the high bunch frequency, this beam can be seen continuously during macropulses. Considering the dose rate of $1.5{\cdot}10^{4}$ Gy/min during macropulses, which is about four orders of magnitudes higher than the mean dose rate, i.e. the dose rate averaged over the irradiation time, the LINAC is often seen to deliver a quasi-continuous beam. The electron beam parameters of the three ELBE pulse regimes, the JETI laser accelerator and the clinical LINAC, are summarized in Table 1.

Experimental set-up for cell irradiation at ELBE

The cell irradiation set-up for radiobiological experiments at ELBE, which is schematically shown in Fig. 2 and previously described in Beyreuther et al. 2015, enabled the online control of beam parameters and dose delivery as well as the remote-controlled irradiation of cell samples. The electron beam generated by the ELBE accelerator was guided to the irradiation room and released from the vacuum tube through a thin beryllium vacuum window (100 μm thick) to enable cell irradiation on air. Then the pencil-like electron beam passed an integrated current transformer (ICT-CF 4.5"/34.9-070-05:1-UHV, Bergoz Instrumentation), which was read out with a 2.5-GHz Digital Phosphor Oscilloscope (DPO 7254; Tektronix) located outside the irradiation room. Following the integrated current transformer, a 5-mm-thick polymethylmethacrylate scatterer was positioned in the beam to ensure the size and homogeneity of the beam spot for irradiation of cell samples with a diameter of 35 mm. Behind the scatterer, the electron beam was either stopped in an in-house-produced aluminium Faraday cup, or passed a cell sample, a phosphorescence screen (Lanex; Kodak) and an ionization chamber (type 10001, sensitive volume 0.6 cm^3, PTW). The Faraday cup was read out with the above-mentioned oscilloscope. The signal of the phosphorescence screen was detected by means of a CCD camera (DMK21BF04; The Imaging Source). During cell irradiation, the Faraday cup and the phosphorescence screen were removed from the electron beam through two remote-controlled linear axes. In beam direction in front of each cell sample, a radiochromic EBT-1 or EBT-2 film (GafChromic, ISP. Corp.) was positioned (Zeil et al. 2009). The cell samples together with the radiochromic films were placed at the ELBE electron beam by an automated cell irradiation system (Zeil et al. 2009). This system enabled the storage of up to 27 cell samples under reduced radiation background by a lead shield of the sample storage container. In addition, the cell irradiation system enabled the separate and remote-controlled transportation of each cell sample into the ELBE electron beam line. The cell samples in beam position were irradiated in vertical orientation in such a way that the horizontal ELBE electron beam passed first through the bottom of the cell culture vessel (1 mm thick, plastic) followed by the cell monolayer (few μm) and finally the cell culture medium (1 cm). In addition to the ionization chamber placed at the central beam axis behind the phosphorescence screen, a second chamber was located on top of the cell sample storage container of the cell irradiation system to monitor the background radiation level. Both ionization chambers were read out with a Unidos electrometer (PTW) placed outside the irradiation room.

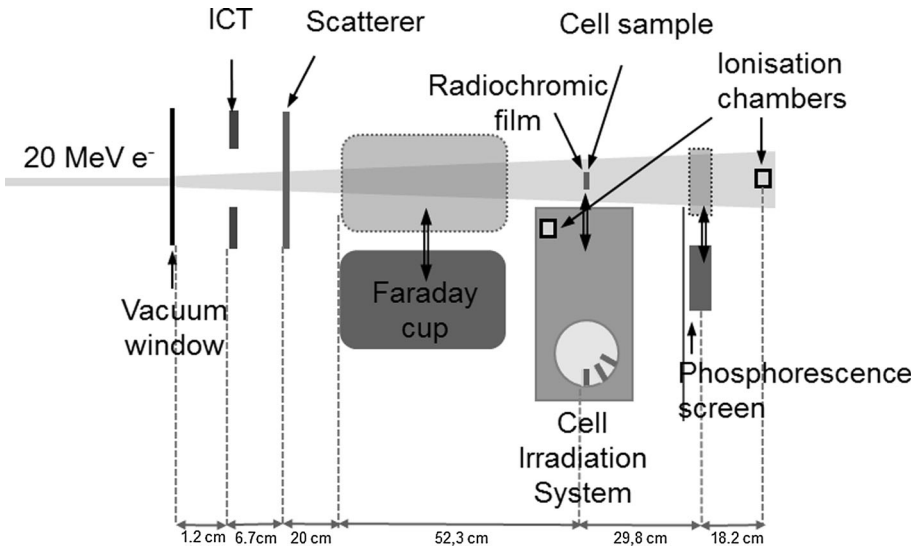

Fig. 2 Schematic illustration of the experimental set-up at the radiation source ELBE. The pencil-like electron beam coming from the accelerator was released from the vacuum tube through a beryllium vacuum window to air and passed subsequently in beam direction through the integrated current transformer (ICT), the scatterer and the cell sample with a radiochromic film in front of the cell sample. Cell samples were stored and separately transported to beam position by the cell irradiation system. The Faraday cup and phosphorescence screen were moved into the beam before, between and after cell irradiation for controlling the electron beam parameters. Two Farmer ionization chambers one fixed at central beam axis and one on the cell irradiation system delivered online information on beam dose and radiation background during cell irradiation, respectively

Beam monitoring, dosimetry and daily experiment procedure at ELBE

The electron beam delivered by the research accelerator ELBE is not as stable as the electron beam provided by a clinical LINAC. The ELBE electron beam intensity, position and spot homogeneity vary from day to day, which complicates the reproducibility of cell irradiation within the experiment campaign of several days distributed over months. Moreover, with regard to a single experimental day, variations in beam position and beam spot homogeneity between the different electron pulse regimes as well as fluctuations of the electron pulse intensity during individual cell irradiation have to be taken into account. Therefore, previously at the laser system JETI established online monitoring of beam parameters and dose delivery as well as determination of absolute doses delivered to individual cell samples (Beyreuther et al. 2010; Richter et al. 2011) were adapted and utilized for the ELBE experiments including a defined experiment procedure that ensures the reproducibility between individual days. The reliability of this dosimetry and beam monitoring system in a daily routine at ELBE was already successfully demonstrated (Beyreuther et al. 2015).

A typical beam time shift at ELBE with a duration of 12 h started with approx. 4-h electron beam tuning by the accelerator crew, followed by around 3-h daily dosimetry including beam monitoring adjustment at the irradiation site, then 4- to 5-h cell irradiation and finally about half an hour constancy check.

The Faraday cup, integrated current transformer, phosphorescence screen and ionization chambers as part of the online dosimetry and beam monitoring system provided data to adjust the electron beam parameters at ELBE to daily measured reference data (for details, see Beyreuther et al. 2015).

After beam tuning, the correlation between the absolute dose measured by radiochromic film at cell position (i.e. in a petri dish replacing the cell monolayer) and the online signal of the ionization chamber at the central beam axis was determined. The resulting correlation factor allowed the online control of dose delivery to the cell monolayer during irradiation by ionization chamber measurement. Additionally, the absolute dose delivery to the cells was retrospectively determined with the radiochromic film in front of each cell sample. Dose deviations between the film position in front of the cell sample and at cell position inside the petri dish were taken into account by simultaneous irradiation of radiochromic films at both positions during daily dosimetry and constancy checks. In this measurement of the film dose ratio between both positions, dose contribution from electron backscattering of the cell culture medium was considered by replacing the cell culture medium with water equivalent solid material (RW3, PTW). For absolute dose determination, the radiochromic films were afore calibrated with a 21-MeV electron beam at

a clinical LINAC and the films were read out with a flatbed scanner (V750pro, Epson) (Richter et al. 2009).

Due to the variation of recombination effects by UHPDR inside the ionization chamber (Karsch et al. 2011; Karsch and Pawelke 2014), the calibration factors between the chamber signal at the central beam axis and the absolute dose provided via radiochromic film at cell position differ for the investigated pulse regimes. Accordingly, the calibration factors were measured for the three pulse regimes independently. The measurement of the calibration factors and of the film dose ratio between both positions was repeated at least three times before starting cell irradiation and at the end of an experimental day for constancy check, respectively.

Due to the very limited beam time availability at the experimental accelerator ELBE and the necessarily extensive physical and dosimetric characterization of the electron beam, the measurement of complete dose–response curves was impossible. Instead, the radiobiological effectiveness of the three electron pulse regimes was determined for the doses 4 and 8 Gy. Moreover, for the primary fibroblasts HDF and F153 only the two pulse regimes UHPDR-HF and the quasi-continuous were investigated.

After beam tuning and dose calibration measurement, it was possible to switch between the three electron pulse regimes (quasi-continuous, UHPDR-LF, and UHPDR-HF) within a few seconds and to deliver prescribed absolute doses to the cells in each pulse regime.

Immunofluorescence detection of DNA DSB

The technique of immunofluorescence staining of the repair proteins γH2AX und 53BP1 was used for the detection of DNA DSB. Directly after irradiation, the cell culture medium was changed and the cell samples were incubated for additional 24 h (37 °C, 5 % CO_2, 95 % humidity) to allow the repair of sublethal damage. The foci that remained 24 h after irradiation were hence defined as residual foci. Subsequently to the incubation, the cell samples were trypsinized and counted. About 2.0×10^5 cells were placed on a glass slide based on cytospin technique for 5 min and 500 g (Cellspin I, Tharmac). The cells on the slides were fixed in 1 % formalin/PBS (phosphate-buffered saline) solution (Merck) for 15 min at room temperature and were washed before immunofluorescence staining once with glycine/PBS (Merck). The permeabilization of the cell membrane occurred with ice-cold triton X-100 solution (0.01 % in PBS v/v, BDH Biochemicals) three times for 5 min. Permeabilized cells were washed in PBGT solution consisting of 0.5 % gelatine (BDH Prolabo®) and 0.025 % TWEEN® 20 (Sigma-Aldrich) in PBS and consecutively stained with anti-phospho-histone H2AX (1:1000 dilution in PBGT, 1 h, upstate), Alexa Fluor® 594 goat anti-mouse IgG (1:400 dilution in PBGT, 30 min, Invitrogen), anti-53BP1 (1:3000 dilution in PBGT, 1 h, Novus Biologicals) and Alexa Fluor® 488 goat anti-rabbit IgG (1:1000 dilution in PBGT, 30 min, Invitrogen). For incubation of each antibody, a 37 °C wet chamber was used. Between the staining steps, the cells on the slides were washed three times with PBGT solution for 5 min, respectively. The cells on the glass slides were mounted with DAPI/Vectashield mounting medium (Vector Laboratories) for visualization of the cell nucleus and were capped with a coverslip. The γH2AX/53BP1 foci were visually analysed by using a fluorescence microscope (Axiovert S100, Carl Zeiss) under 1000-fold magnification with a N-Achroplan 100×1.25 Oil Ph3 objective (NA = 0.17; Carl Zeiss) and an "HC Tripleband-Filterset DAPI/FITC/TxRED" (AHF Analysentechnik). For dose point evaluation randomly chosen 100 intact nuclei were analysed that was controlled by DAPI staining.

Colony-forming assay

For analysing the clonogenic survival, the standard colony-forming assay was used. Immediately after irradiation, the cells were trypsinized and seeded for each dose point in 6 different concentrations using 6-well plates (Greiner bio one). The seeded cells were incubated (37 °C, 5 % CO_2, 95 % humidity) for 13 days. After incubation, the cells were fixed with ice-cold 80 % ethanol for 15 min and stained with crystal violet (Clin-Tec) for further 10 min. Colonies consisting of more than 50 cells were accounted for analysis and therewith considered as survivor. The analysis of colonies was performed by using a microscope (Axiovert S100, Carl Zeiss) under 40-fold magnification. The surviving fractions of irradiated cells were ascertained by normalization to non-irradiated cells which were used as controls.

Data processing and statistical analysis

To compare the different ELBE electron pulse regimes, at least three independent experiment replications each with not less than two samples were performed for each electron pulse regime, dose point, cell line and biological endpoint under investigation. However, varying beam parameters between different pulse regimes and individual sample irradiation result in dose rate variations of about 10 % within and between experiment sessions and, finally, in noticeable deviations from the requested dose (for details, see Beyreuther et al. 2015). Approximating the scheduled doses of 4 Gy and 8 Gy, individual dose values (D_i) in the ranges of 3.18–4.73 Gy and 7.40–10.70 Gy, respectively, were retrospectively determined for individual cell samples. In consequence, the biological results of the three

experiment replications were not combined by averaging before any fit procedure but considered as individual findings (surviving fraction SF_i or number of foci F_i) with their appendant dose values (D_i). This treatment as distinct measurements results in more data points with a broader dose range than the originally planned two single dose points for the determination of dose–response curves.

Assuming the generally accepted dose dependencies for low linear energy transfer radiation, the measured surviving fractions after irradiation with the different ELBE electron pulse regimes were fitted by using the linear quadratic equation $SF(D) = 100\ \exp(-\alpha D - \beta D^2)$, with SF as surviving fraction in dependence on dose D and α as well as β as fitting parameters. For analysing the yields of residual γH2AX/53BP1 foci, the background levels determined by control cell samples were first subtracted from every data point of the irradiated cell samples. The resulting number of γH2AX/53BP1 foci (F) in dependence on dose D was fitted with the linear model $F(D) = \alpha D$, with α as the fitting parameter.

The fit procedures were performed with the software Origin 8.1 (OriginLab Corporation, Northampton USA), which allows to include the uncertainty in one dimension in a weighted least squares minimization. However, in the present work every data point has biological uncertainties (ΔSF_i or ΔF_i), which consider systematic errors of the laboratory process and uncertainties of the measured biological endpoints, and dose uncertainties ΔD_i, which were individually determined for each electron-irradiated sample taking into account the dose inhomogeneity over the sample area as measured by radiochromic films and the uncertainty of the film calibration (Richter et al. 2009, 2011). Therefore, the fit procedure was split in two stages. In the first fit, only the biological uncertainties of the measured values (ΔSF_i or ΔF_i) were included as weights. For the second stage, the dose errors (ΔD_i) were included by calculating combined uncertainties (ΔSFD_i or ΔFD_i) for each data point, assuming Gaussian error propagation with the equation parameters determined in the first stage. Then, the fit was repeated now using ΔSFD_i and ΔFD_i as weights, respectively. On basis of this fit procedure, the final fit parameters, the dose–response curves and the 95 % confidence intervals were calculated.

For representation, all measured values SF_i and F_i were depicted with their appendant biological (ΔSF_i or ΔF_i) and dose (ΔD_i) uncertainties (Figs. 3, 4, 5).

Results

The influence of very short pulses with UHPDR as one specific property of laser-accelerated particle beams on the in vitro radiobiological outcome was investigated at the

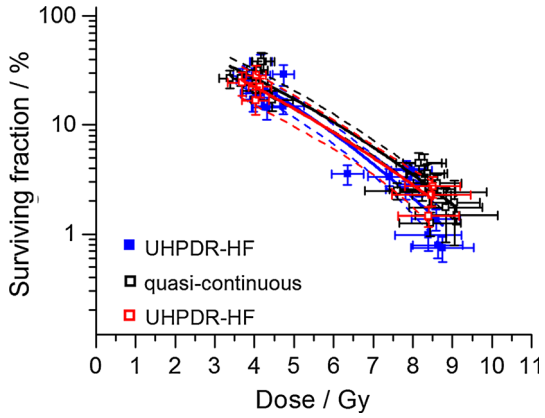

Fig. 3 Clonogenic survival of the normal tissue cell line 184A1 after electron irradiation with the ELBE pulses of the UHPDR-LF (*red*) and UHPDR-HF (*blue*) regime and with a quasi-continuous beam (*black*). The *solid lines* are the results of the curve fitting, and the *dashed lines* correspond to the 95 % confidence intervals of the model function after curve fitting. The results of individual sample irradiations are depicted as *squares* together with their associated biological and dose uncertainties (colour figure online)

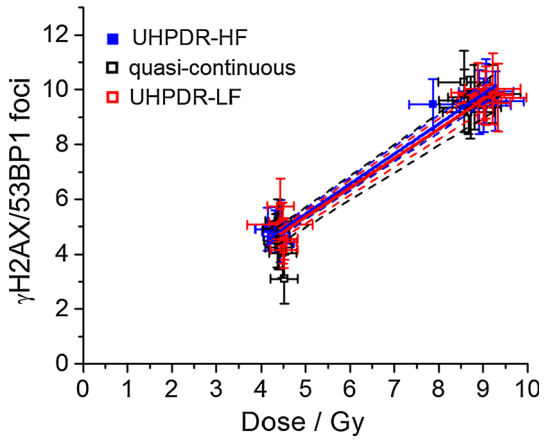

Fig. 4 Residual DNA DSB that remain 24 h after treatment with the UHPDR-LF (*red*), UHPDR-HF (*blue*) and quasi-continuous (*black*) ELBE electron beam regime for the normal tissue cell line 184A1. As a result of the curve fitting, the dose–response *curves* are represented as *solid lines* and the 95 % confidence intervals as *dashed lines*, respectively; the result of each individual sample with their appendant biological and dose uncertainties is shown as *square* (colour figure online)

radiation source ELBE. The allocable experimental shifts at the ELBE accelerator extended over a time period of 2 years, whereas in total 147 cell samples were irradiated and a multiple amount of control samples were carried in sham irradiation.

The radiobiological results for the clonogenic survival caused by the three ELBE electron pulse regimes in the normal tissue cell line 184A1 are shown in Fig. 3. The corresponding dose–response function parameters resulting from the regression are listed in Table 2. For all three ELBE electron beam pulse regimes, no clear differences in

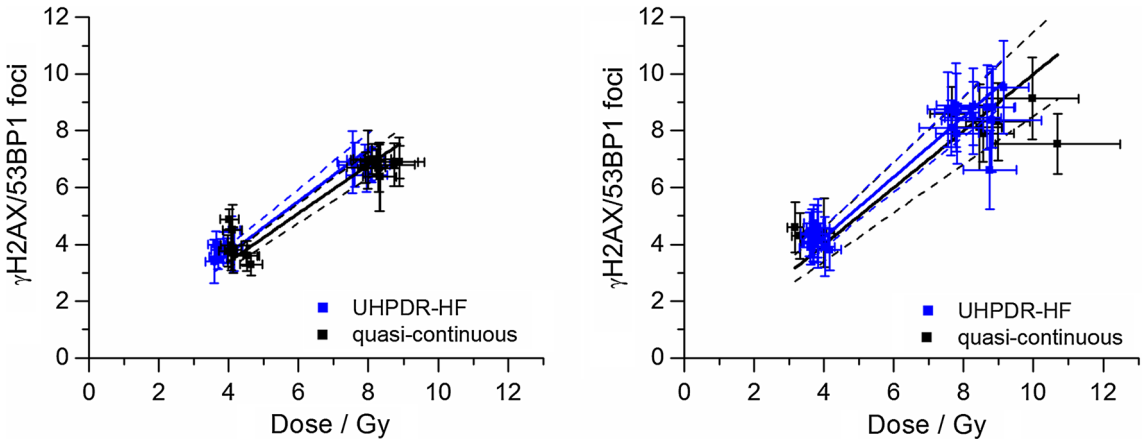

Fig. 5 Residual DNA DSB that remain 24 h after dose application of 4 and 8 Gy with the ELBE electron beam regime UHPDR-HF (*blue*) and quasi-continuous (*black*) for the primary fibroblasts HDF (*left*) and F153 (*right*). The fitted dose–response curves (*solid lines*) were shown together with their 95 % confidence intervals (*dashed lines*); the underlying results of individual sample irradiation are represented by *squares* together with their associated biological and dose uncertainties (colour figure online)

Table 2 Fit parameter (±SE) and coefficient of determination for the linear quadratic survival curves of cell line 184A1 presented in Fig. 3

Beam pulse regime	α/Gy^{-1}	β/Gy^{-2}	R^2
Quasi-continuous	0.218 ± 0.055	0.032 ± 0.008	0.821
UHPDR-HF	0.236 ± 0.048	0.023 ± 0.005	0.829
UHPDR-LF	0.299 ± 0.062	0.018 ± 0.008	0.912

Table 3 Fit parameter (±SE) and coefficient of determination for the linear dose–response curves for residual DNA DSB of cell line 184A1 presented in Fig. 4

Beam pulse regime	α/Gy^{-1}	R^2
Quasi-continuous	1.069 ± 0.034	0.989
UHPDR-HF	1.093 ± 0.018	0.997
UHPDR-LF	1.071 ± 0.021	0.996

the clonogenic survival were observed within the 95 % confidence intervals. The results of the second biological endpoint the residual DNA DSB are shown for the normal tissue cell line 184A1 after irradiation with the three ELBE electron pulse regimes in Fig. 4. The corresponding function parameters resulting from the curve fitting are listed in Table 3. As already ascertained for the clonogenic survival, no considerable differences in the radiobiological effectiveness after irradiation with each pulse regime were revealed for the dose-dependent number of residual γH2AX/53BP1 double-positive foci under consideration of the 95 % confidence intervals. The results obtained for the additionally investigated human primary fibroblasts HDF and F153 were quite similar, showing no clear dose regime difference for the dose-dependent number of γH2AX/53BP1 double-positive foci within the 95 % confidence intervals (Fig. 5). The appendant function parameters resulting from the curve fitting are listed in Table 4.

Table 4 Fit parameter (±SE) and coefficient of determination for the linear dose–response curves for residual DNA DSB of primary fibroblasts presented in Fig. 5

Cell line	Beam pulse regime	α/Gy^{-1}	R^2
HDF	Quasi-continuous	0.847 ± 0.027	0.980
	UHPDR-HF	0.918 ± 0.032	0.989
F153	Quasi-continuous	1.061 ± 0.043	0.989
	UHPDR-HF	0.999 ± 0.064	0.965

Discussion

Motivated by the development and establishment of laser-based particle accelerators for a future medical application, the presented radiobiological in vitro experiments were realized with the objective to investigate the influence of UHPDR as radiobiological important specific property of laser-driven beams. The experiments were performed at the experimental radiation source ELBE that enabled to mimic the electron pulses with UHPDR of the laser accelerator JETI and the quasi-continuous electron beam of a clinical LINAC, both used in separated experiment campaign in a previous study (Laschinsky et al. 2012). Thus, the radiobiological effects of both electron pulse regimes could be studied in one experimental campaign and at one irradiation system, i.e. using the same set-up and dosimetry, reducing influences on the radiobiological outcome arising from non-radiation effects and systematic uncertainties

because of different dose measurements and different other beam properties.

With regard to the 95 % confidence intervals, the results of the presented experiments showed that a UHPDR up to 10^{10} Gy/min and a mean dose rate in the range of $\sim$0.4–10^{6} Gy/min (Table 1) neither for clonogenic survival (Fig. 3) nor for residual DNA DSB (Fig. 4) led to a change in the radiobiological effectiveness for the human normal tissue cell line 184A1. Based on the results for both investigated endpoints in the present experiment, there is no evidence for relevance whether the irradiation occurs with a quasi-continuous beam analogue to irradiation with a clinical LINAC or with a pulsed beam of UHPDR-LF analogue to the laser accelerator JETI. Also an increase in the frequency of pulses with UHPDR (UHPDR-HF) and the corresponding delivery of the total dose within a single short macropulse of few hundred microseconds duration results not in a noticeable difference of the clonogenic survival or number of residual DNA DSB. The additionally performed experiments with both primary fibroblasts HDF and F153 (Fig. 5) showed also no obvious difference in the radiobiological outcome for residual DNA DSB between quasi-continuous and UHPDR-HF electron pulse regimes at ELBE, confirming the radiobiological results for the normal tissue cell line 184A1.

This finding is in accordance with the results of experiments performed in parallel to this study at the radiation source ELBE, investigating the radiobiological outcome of the three electron pulse regimes for two head and neck tumour cell lines of different radiosensitivity (Beyreuther et al. 2015). Also no significant difference in the radiobiological effectiveness for both tumour cell lines was determined for the biological endpoints clonogenic survival and residual DNA DSB.

Further in vitro studies on the radiobiological influence of UHPDR have been performed with short single pulses of conventional electron accelerators (Berry and Stedeford 1972; Purrott and Reeder 1977; Purdie et al. 1980; Cygler et al. 1994; DeVeaux et al. 2006). The mentioned pulse dose rates of $\leq 10^{13}$ Gy/min showed overall no influence on the radiobiological outcome even if the comparability of these studies is limited by the use of different experiment parameters within one study, e.g. corresponding reference radiation quality.

In line with the mentioned studies, no influence for the number of residual γ-H2AX foci (Sato et al. 2010) and the clonogenic survival (Tillman et al. 1999; Shinohara et al. 2004) was detected by comparing the irradiation with laser-generated ultra-short soft X-ray pulses of UHPDR of up to 10^{15} Gy/min, as ditto a low LET beam quality, and continuous reference irradiation. More recently, the determination of the radiobiological response of pulsed and continuous proton beams generated by a conventional tandem accelerator showed no difference in the radiobiological effectiveness regarding micronucleus induction (Schmid et al. 2009, 2010), cell killing (Auer et al. 2011) and number of radiation-induced DNA DSB (Zlobinskaya et al. 2012). Also the first investigations with laser-accelerated proton pulses indicated no influence of UHPDR on the radiobiological effectiveness (Yogo et al. 2011; Bin et al. 2012; Doria et al. 2012; Zeil et al. 2013). Even if these results for proton beams cannot necessarily be transferred to electron irradiation, they are supporting the finding of the presented experiments of a comparable radiobiological effectiveness of conventional and laser-accelerated electron beams. In this context, the deposited energy or dose per pulse should be mentioned, which was in the order of a few Gy for all single shot trials (Berry and Stedeford 1972; Purrott and Reeder 1977; Purdie et al. 1980; Cygler et al. 1994; Shinohara et al. 2004; DeVeaux et al. 2006; Yogo et al. 2011; Bin et al. 2012; Doria et al. 2012). On the other hand, pulse doses of a few mGy comparable to the macropulse dose of a clinical LINAC were delivered in the present work and in some of the electron (Tillman et al. 1999; Sato et al. 2010; Laschinsky et al. 2012) and proton studies (Zeil et al. 2013). Anyhow, as in no case an altered radiobiological response to the treatment with the varying experimental accelerators was found, the influence of dose per pulse might be insignificant or superimposed by comparable pulse dose rates.

In contrast to all above-mentioned studies, a significant decrease in the micronuclei yield with increasing dose rates per pulse was observed, when dose was delivered by a single electron pulse (a few Gy) of a modern classic radiotherapy device (Acharya et al. 2011). However, within the same study no reduction in the micronuclei yield was detected when the dose was delivered by multiple electron pulses (Acharya et al. 2011).

In summary, the previously reported significantly reduced radiobiological effectiveness of a laser-accelerated electron beam (Laschinsky et al. 2012), measured only for the normal tissue cell line 184A1 and only for the biological endpoint residual DNA DSB, cannot be conclusively clarified. Apart from UHPDR, further conceivable influence factors, such as energy spectrum, low mean dose rate and non-radiation-induced biological effects, have been excluded. Nevertheless, the results of the present study as well as the published data of other studies indicate that the specific property of laser-accelerated electron beams (short pulses with UHPDR of $\sim 10^{10}$ Gy/min) alone leads to no modification of the radiobiological effectiveness of the probed cell cultures.

The radiobiological characterization of UHPDR within the present study used cell monolayer cultures that represent a simple biological system. To come closer to the clinical situations of tumours with their specific

environment, irradiation experiments with higher-order organisms of more complex physiology are required. Concerning this matter, an in vivo study demonstrated a differential response between normal and tumour tissue after irradiation with a pulsed, ultra-high dose rate electron beam (a few Gy in 1-μs single pulse) compared to a continuous, conventional electron beam delivered by a conventional experimental linear accelerator (Favaudon et al. 2014). More recently, an in vivo irradiation campaign was set-up at a laser-accelerated electron beam to investigate the radiation-induced growth delay of a human tumour using a nude mice model (Schürer et al. 2012; Brüchner et al. 2014). Within this study, no significant difference in the radiobiological outcome after irradiation with the laser-accelerated electron beam of UHPDR ($\sim 10^{12}$ Gy/min, $\leq$80 mGy/$\sim$1 ps) compared to the quasi-continuous reference electron beam delivered by a clinical LINAC was demonstrated (Oppelt et al. 2015). In a first in vivo trial with protons, Zlobinskaya et al. (2014) reveal no difference in tumour growth delay between continuous and ultra-short-pulsed proton beams ($\leq$20 Gy/1 ns) at a conventional tandem accelerator. Particularly with regard to the study of Favaudon et al. 2014, there are further needs of irradiation experiments in vivo with laser-accelerated particle beams investigating normal tissue response.

Acknowledgments The authors are much obligated to the ELBE crew for their continuing interest and support of the presented study. The work was supported by the German Government, Federal Ministry of Education and Research, Grant Nos. 03ZIK445 and 03Z1N511.

Compliance with ethical standards

Conflicts of interest The authors declare that they have no conflict of interests.

Human and animal right statement This article does not contain any studies with human participants or animals performed by any of the authors.

References

Acharya S, Bhat NN, Joseph P, Sanjeev G, Sreedevi B, Narayana Y (2011) Dose rate effect on micronuclei induction in human blood lymphocytes exposed to single pulse and multiple pulses of electrons. Radiat Environ Biophys 50:253–263. doi:10.1007/s00411-011-0353-1

Auer S, Hable V, Greubel C, Drexler GA, Schmid TE, Belka C, Dollinger G, Friedl AA (2011) Survival of tumor cells after proton irradiation with ultra-high dose rates. Radiat Oncol 6:139. doi:10.1186/1748-717X-6-139

Berry RJ, Stedeford JB (1972) Reproductive survival of mammalian cells after irradiation at ultra-high dose-rates: further observations and their importance for radiotherapy. Br J Radiol 45:171–177. doi:10.1259/0007-1285-45-531-171

Beyreuther E, Lessmann E, Pawelke J, Pieck S (2009) DNA double-strand break signalling: X-ray energy dependence residual co-localised foci of gamma-H2AX and 53BP1. Int J Radiat Biol 85:1042–1050. doi:10.3109/09553000903232884

Beyreuther E, Enghardt W, Kaluza M, Karsch L, Laschinsky L, Lessmann E, Nicolai M, Pawelke J, Richter C, Sauerbrey R, Schlenvoigt HP, Baumann M (2010) Establishment of technical prerequisites for cell irradiation experiments with laser-accelerated electrons. Med Phys 37:1392–1400. doi:10.1118/1.3301598

Beyreuther E, Karsch L, Laschinsky L, Lessmann E, Naumburger D, Oppelt M, Richter C, Schürer M, Woithe J, Pawelke J (2015) Radiobiological response to ultra-short pulsed megavoltage electron beams of ultra-high pulse dose rate. Int J Radiat Biol 91:643–652. doi:10.3109/09553002.2015.1043755

Bin J, Allinger K, Assmann W, Dollinger G, Drexler GA, Friedl AA, Habs D, Hilz P, Hoerlein R, Humble N, Karsch S, Khrennikov K, Kiefer D, Krausz F, Ma W, Michalski D, Molls M, Raith S, Reinhardt S, Röper B, Schmid TE, Tajima T, Wenz J, Zlobinskaya O, Schreiber J, Wilkens JJ (2012) A laser-driven nanosecond proton source for radiobiological studies. Appl Phys Lett 101:243701. doi:10.1063/1.4769372

Brüchner K, Beyreuther E, Baumann M, Krause M, Oppelt M, Pawelke J (2014) Establishment of a small animal tumour model for in vivo studies with low energy laser accelerated particles. Radiat Oncol 9:57. doi:10.1186/1748-717X-9-57

Cygler J, Klassen NV, Ross CK, Bichay TJ, Raaphorst GP (1994) The survival of aerobic and anoxic human glioma and melanoma cells after irradiation at ultrahigh and clinical dose rates. Radiat Res 140:79–84. doi:10.2307/3578571

DeVeaux LC, Wells DP, Hunt A, Webb T, Beezhold W, Harmon JF (2006) Accelerator-based radiation sources for next-generation radiobiological research. Nucl Instr Methods Phys Res A 562:981–984. doi:10.1016/j.nima.2006.02.119

Doria D, Kakolee KF, Kar S, Litt SK, Fiorini F, Ahmed H, Green S, Jeynes JCG, Kavanagh J, Kirby D, Kirkby KJ, Lewis CL, Merchant MJ, Nersisyan G, Prasad R, Prise KM, Schettino G, Zepf M, Borghesi M (2012) Biological effectiveness on live cells of laser driven protons at dose rates exceeding 10^9 Gy/s. AIP Adv 2:011209. doi:10.1063/1.3699063

Favaudon V, Caplier L, Monceau V, Pouzoulet F, Sayarath M, Fouillade C, Poupon MR, Brito I, Hupé P, Bourhis J, Hall J, Fontaine JJ, Vozenin MC (2014) Ultrahigh dose-rate FLASH irradiation increases the differential response between normal and tumor tissue in mice. Sci Transl Med 6:245ra93. doi:10.1126/scitranslmed.3008973

Gabriel F, Gippner P, Grosse E, Janssen D, Michel P, Prade H, Schamlott A, Seidel W, Wolf A, Wünsch R, ELBE-crew (2000) The Rossendorf radiation source ELBE and its FEL projects. Nucl Instrum Methods B 161:1143–1147. doi:10.1016/S0168-583X(99)00909-X

Karsch L, Pawelke J (2014) Theoretical investigation of the saturation correction for ionization chambers irradiated with pulsed beams of arbitrary pulse length. Z Med Phys 24:201–210. doi:10.1016/j.zemedi.2013.10.007

Karsch L, Richter C, Pawelke J (2011) Experimentelle Untersuchung der Sättigungskorrelation einer PTW Roos-Ionisationskammer in gepulsten Strahlungsfeldern mit hoher Pulsdosis bei verschiedenen Pulsdauern. Z Med Phys 21:4–10. doi:10.1016/j.zemedi.2010.10.008

Kraft SD, Richter C, Zeil K, Baumann M, Beyreuther E, Bock S, Bussmann M, Cowan TE, Dammene Y, Enghardt W, Helbig U, Karsch L, Kluge T, Laschinsky L, Leßmann E, Metzkes J, Naumburger D, Sauerbrey R, Schürer M, Sobiella M, Woithe J, Schramm U, Pawelke J (2010) Dose-dependent biological damage of tumour cells by laser-accelerated proton beams. New J Phys 12:085003. doi:10.1088/1367-2630/12/8/085003

Labate L, Andreassi MG, Baffigi F, Basta G, Bizzarri R, Borghini A, Candiano GC, Casarino C, Cresci M, Martino FD, Fulgentini L,

Ghetti F, Gilardi MC, Giulietti A, Köster P, Lenci F, Levato T, Oishi Y, Russo G, Sgarbossa A, Traino C, Gizzi LA (2013) Small-scale laser based electron accelerators for biology and medicine: a comparative study of the biological effectiveness. In: Proceedings of SPIE, p 8779. doi: 10.1117/12.2019689

Laschinsky L, Baumann M, Beyreuther E, Enghardt W, Kaluza M, Karsch L, Lessmann E, Naumburger D, Nicolai M, Richter C, Sauerbrey R, Schlenvoigt HP, Pawelke J (2012) Radiobiological effectiveness of laser accelerated electrons in comparison to electron beams from a conventional linear accelerator. J Radiat Res 53:395–403. doi:10.1269/jrr.11080

Ledingham KWD, Galster W, Sauerbrey R (2007) Laser-driven proton oncology—a unique new cancer therapy. Br J Radiol 80:855–858. doi:10.1259/bjr/29504942

Linz U, Alonso J (2007) What will it take for laser driven proton accelerators to be applied to tumor therapy? Phys Rev Spec Accel Beams 10:094801. doi:10.1103/PhysRevSTAB.10.094801

Lundh O, Rechatin C, Faure J, Ben-Ismaïl A, Lim J, De Wagter C, De Neve W, Malka V (2012) Comparison of measured with calculated dose distribution from a 120-MeV electron beam from a laser-plasma accelerator. Med Phys 39:3501–3508. doi:10.1118/1.4719962

Michaels HB, Epp ER, Ling CC, Peterson EC (1978) Oxygen sensitization of CHO cells at ultrahigh dose rates: prelude to oxygen diffusion studies. Radiat Res 76:510–521. doi:10.2307/3574800

Oppelt M, Baumann M, Bergmann R, Beyreuther E, Brüchner K, Hartmann J, Karsch L, Krause M, Laschinsky L, Leßmann E, Nicolai M, Reuter M, Richter C, Sävert A, Schürer M, Schnell M, Woithe J, Kaluza M, Pawelke J (2015) Comparison study of in vivo dose response to laser-driven versus conventional electron beam. Radiat Environ Biophys 54:155–166. doi:10.1007/s00411-014-0582-1

Purdie JW, Inhaber ER, Klassen NV (1980) Increased sensitivity of mammalian cells irradiated at high dose rates under oxic conditions. Int J Radiat Biol Relat Stud Phys Chem Med 37:331–335

Purrott RJ, Reeder EJ (1977) Chromosome aberration yields induced in human lymphocytes by 15 MeV electrons given at a conventional dose-rate and in microsecond pulses. Int J Radiat Biol Relat Stud Phys Chem Med 31:251–256. doi:10.1080/09553007714550291

Richter C, Pawelke J, Karsch L, Woithe J (2009) Energy dependence of EBT-1 radiochromic film response for photon (10 kVp–15 MVp) and electron beams (6–18 MeV) readout by a flatbed scanner. Med Phys 36:5506–5514. doi:10.1118/1.3253902

Richter C, Kaluza M, Karsch L, Schlenvoigt HP, Schürer M, Sobiella M, Woithe J, Pawelke J (2011) Dosimetry of laser-accelerated electron beams used for in vitro cell irradiation experiments. Radiat Meas 46:2006–2009. doi:10.1016/j.radmeas.2011.04.019

Rigaud O, Fortunel NO, Vaigot P, Cadio E, Martin MT, Lundh O, Faure J, Rechatin C, Malka V, Gauduel YA (2010) Exploring ultrashort high-energy electron-induced damage in humane carcinoma cells. Cell Death Dis 1:e73. doi:10.1038/cddis.2010.46

Sato K, Nishikino M, Okano Y, Ohshima S, Hasegawa N, Ishino M, Kawachi T, Numasaki H, Teshima T, Nishimura H (2010) γ-H2AX and phosphorylated ATM focus formation in cancer cells after laser plasma X irradiation. Radiat Res 174:436–445. doi:10.1667/RR2178.1

Schmid TE, Dollinger G, Hauptner A, Hable V, Greubel C, Auer S, Friedl AA, Molls M, Röper B (2009) No evidence for a different RBE between pulsed and continuous 20 MeV protons. Radiat Res 172:567–574. doi:10.1667/RR1539.1

Schmid TE, Dollinger G, Hable V, Greubel C, Zlobinskaya O, Michalski D, Molls M, Röper B (2010) Relative biological effectiveness of pulsed and continuous 20 MeV protons for micronucleus induction in 3D human reconstructed skin tissue. Radiother Oncol 95:66–72. doi:10.1016/j.radonc.2010.03.010

Schürer M, Baumann M, Beyreuther E, Brüchner K, Enghardt W, Kaluza M, Karsch L, Laschinsky L, Leßmann E, Nicolai M, Oppelt M, Reuter M, Richter C, Sävert A, Schnell M, Woithe J, Pawelke J (2012) Irradiation system for pre-clinical studies with laser accelerated electrons. Biomed Tech 57(Suppl. 1):62–65. doi:10.1515/bmt-2012-4244

Shinohara K, Nakano H, Miyazaki N, Tago M, Kodama R (2004) Effects of single-pulse (≤1 ps) X-rays from laser-produced plasmas on mammalian cells. J Radiat Res 45:509–514. doi:10.1269/jrr.45.509

Stampfer MR, Bartley JC (1985) Induction of transformation and continuous cell lines from normal human mammary epithelial cells after exposure to benzo[a]pyrene. Proc Natl Acad Sci USA 82:2394–2398

Tillman C, Grafström G, Jonsson AC, Jönsson BA, Mercer I, Mattsson S, Strand SE, Svanberg S (1999) Survival of mammalian cells exposed to ultrahigh dose rates from a laser-produced plasma x-ray source. Radiology 213:860–865. doi:10.1148/radiology.213.3.r99dc13860

Yogo A, Maeda T, Hori T, Sakaki H, Ogura K, Nishiuchi M, Sagisaka A, Kiriyama H, Okada H, Kanazawa S, Shimomura T, Nakai Y, Tanoue M, Sasao F, Bolton PR, Murakami M, Nomura T, Kawanishi S, Kondo K (2011) Measurement of relative biological effectiveness of protons in human cancer cells using laser-driven quasimonoenergetic proton beamline. Appl Phys Lett 98:053701. doi:10.1063/1.3551623

Zeil K, Beyreuther E, Lessmann E, Wagner W, Pawelke J (2009) Cell irradiation setup and dosimetry for radiobiological studies at ELBE. Nucl Instrum Meth Phys Res B 267:2403–2410. doi:10.1016/j.nimb.2009.04.015

Zeil K, Baumann M, Beyreuther E, Burris-Mog T, Cowan TE, Enghardt W, Karsch L, Kraft SD, Laschinsky L, Metzkes J, Naumburger D, Oppelt M, Richter C, Sauerbrey R, Schürer M, Schramm U, Pawelke J (2013) Dose-controlled irradiation of cancer cells with laser accelerated proton pulses. Appl Phys B 110:437–444. doi:10.1007/s00340-012-5275-3

Zlobinskaya O, Dollinger G, Michalski D, Hable V, Greubel C, Du G, Multhoff G, Röper B, Molls M, Schmid TE (2012) Induction and repair of DNA double-strand breaks assessed by gamma-H2AX foci after irradiation with pulsed or continuous proton beams. Radiat Environ Biophys 51:23–32. doi:10.1007/s00411-011-0398-1

Zlobinskaya O, Siebenwirth C, Greubel C, Hable V, Hertenberger R, Humble N, Reinhardt S, Michalski D, Röper B, Multhoff G, Dollinger G, Wilkens JJ, Schmid TE (2014) The effects of ultra-high dose rate proton irradiation on growth delay in the treatment of human tumor xenografts in nude mice. Radiat Res 181(2):177–183. doi:10.1667/RR13464.1